

Organ Morphogenesis in the Chicken Inner Ear

Weise Chang,* Fabio D. Nunes,* Jose M. De Jesus-Escobar,†
Richard Harland,† and Doris K. Wu*¹

*National Institute on Deafness and Other Communication Disorders, Rockville, Maryland 20850; and †Department of Molecular and Cell Biology, Division of Biochemistry and Molecular Biology, University of California, Berkeley, Berkeley, California 94720

Bone morphogenetic protein 4 (Bmp4) is expressed during multiple stages of development of the chicken inner ear. At the otocyst stage, Bmp4 is expressed in each presumptive sensory organ, as well as in the mesenchymal cells surrounding the region of the otocyst that is destined to form the semicircular canals. After the formation of the gross anatomy of the inner ear, Bmp4 expression persists in some sensory organs and restricted domains of the semicircular canals. To address the role of this gene in inner ear development, we blocked BMP4 function(s) by delivering one of its antagonists, Noggin, to the developing inner ear *in ovo*. Exogenous Noggin was delivered to the developing otocyst by using a replication-competent avian retrovirus encoding the *Noggin* cDNA (RCAS-N) or implanting beads coated with Noggin protein. Noggin treatment resulted in a variety of phenotypes involving both sensory and nonsensory components of the inner ear. Among the nonsensory structures, the semicircular canals were the most sensitive and the endolymphatic duct and sac most resistant to exogenous Noggin. Noggin affected the proliferation of the primordial canal outpouch, as well as the continual outgrowth of the canal after its formation. In addition, Noggin affected the structural patterning of the cristae, possibly via a decrease of *Msx1* and *p75NGFR* expression. These results suggest that BMP4 and possibly other BMPs are required for multiple phases of inner ear development. © 1999 Academic Press

Key Words: bone morphogenetic proteins; TUNEL; vestibule; *Msx1*; *p75NGFR*.

INTRODUCTION

The vertebrate inner ear is a remarkably complex organ consisting of several precisely arranged components of sensory and nonsensory origins. As a step toward unraveling molecular mechanisms underlying the formation of such a complex organ, the temporal and spatial patterns of expression of many genes have been examined in the developing inner ear (for review, see Torres and Giraldez, 1998; Fritzsche *et al.*, 1998). In addition, using the gene targeting approach in mice, several of these genes have been demonstrated to be essential for the proper formation of the inner ear (for review, see Fekete, 1999). For example, knockouts of the mouse *Pax2* and *Hmx3* (*Nkx5.1*) genes affect the formation of the cochlea and vestibular components of the inner ear, respectively (Torres *et al.*, 1996; Wang *et al.*,

1998; Hadrys *et al.*, 1998), while absence of the *Otx1* gene results in the loss of the lateral canal and ampulla, as well as defects in the shape of the cochlea (Acampora *et al.*, 1996; Morsli *et al.*, 1999).

BMP4 was originally isolated from bone based on its ability to induce ectopic bone formation (Urist *et al.*, 1979; Wozney *et al.*, 1988). Since then, it has become evident that BMP4 plays several critical roles during embryogenesis mediating the development of multiple organs (for review, see Hogan, 1996; Cho and Blitz, 1998). In many of these organs such as the neural tube (McMahon *et al.*, 1998), limbs (Capdevila and Johnson, 1998; Brunet *et al.*, 1998; Pizette and Niswander, 1999), somites (McMahon *et al.*, 1998; Reshef *et al.*, 1998; Marcelle *et al.*, 1997), and possibly heart (Schultheiss *et al.*, 1997), BMP4 interacts with one of its antagonists, Noggin, in a coordinated fashion to generate normal structural patterning and cellular differentiation.

Noggin is a secreted glycoprotein that was identified based on its ability to mimic the Spemann organizer in promoting dorsal mesodermal structures and neural induc-

¹ To whom correspondence should be addressed at NIDCD, 5 Research Court, Room 2B34, Rockville, MD 20850. Fax: (301) 402-3470. E-mail: wud@nidcd.nih.gov.

tion in *Xenopus* (Smith and Harland, 1992). In mice, *Noggin* is not required for neural induction, however, it is important for the growth and patterning of the neural tube and somites (McMahon *et al.*, 1998). *Noggin* acts by binding to BMP4 and BMP2 with high affinity (dissociation constant in the picomolar range), thus preventing these proteins from interacting with their putative receptors (Zimmerman *et al.*, 1996; Holley *et al.*, 1996).

Previously, we have shown that *Bmp4* is expressed in the three presumptive cristae in mice and in all eight presumptive sensory organs (the basilar papilla, macula utriculi, macula sacculi, three cristae, lagena, and macula neglecta) in chicken (Morsli *et al.*, 1998; Wu and Oh, 1996). In the chicken inner ear, *Bmp4* is initially expressed in the medial and posterior margins of the invaginating otic cup, and its expression becomes restricted to two foci in the otocyst. These two foci correspond to the location of the future anterior and posterior cristae. This early pattern of *Bmp4* expression is conserved among chicken, mouse, and *Xenopus* (Wu and Oh, 1996; Morsli *et al.*, 1998; Hemmati-Briuanlou and Thomsen, 1995). In later stages of otocyst development, *Bmp4* expression diverges between chicken and mice, being expressed in the sensory tissues of the cochlea (basilar papilla), utricle, and saccule of chicken, but not those of the mouse. Also, at these later stages, *Bmp4* is expressed in the otic epithelium and its adjacent mesenchymal region that is destined to form the semicircular canals in both chicken and mouse (Oh *et al.*, 1996; unpublished results). The conserved patterns of *Bmp4* expression in early stages of inner ear development among different species and the important role of *Bmp4* in embryogenesis of other organs suggest that BMP4 is essential for the normal development of the inner ear. Unfortunately, this hypothesis cannot be easily tested in the *Bmp4* knockout mouse model since these mice die shortly after otocyst formation (Winnier *et al.*, 1995). In this study, we investigated the function(s) of BMP4 during chicken inner ear development by ectopic expression of *Noggin* using a replication-competent retrovirus encoding *Noggin* or beads coated with *Noggin* protein. Our results show that blocking endogenous BMP4 and possibly other BMPs *in vivo* resulted in malformations of both sensory and nonsensory components of the inner ear. Furthermore, we provide evidence that there is a continual requirement of BMP(s) during canal formation and the growth phase after the canals are formed.

MATERIALS AND METHODS

Chicken Embryos

Fertilized White Leghorn eggs (Spafas, CT) were incubated at 38°C. Embryos were staged according to Hamburger and Hamilton (1951) prior to viral injection or implantation and sacrificed at designated times after operations.

Preparation of *Noggin* Expressing Virus

Replication-competent avian sarcoma retroviral vector encoding the chicken *Noggin* cDNA (RCAS-N) was a gift of Randy Johnson (Capdevila and Johnson, 1998). Virus stocks were prepared by transfecting plasmids into line-0 chicken embryo fibroblasts, and media were collected and concentrated as described (Morgan and Fekete, 1996). The titers of virus stocks were 1.3×10^8 and 0.9×10^8 infectious units/ml for RCAS-N and RCAS-N-ro (RCAS encoding *Noggin* cDNA cloned in a reverse orientation as a control), respectively. Viruses were injected into either the lumen of the otocyst or its surrounding mesenchyme. For injections from E2.5 to E4, a volume of approximately 50–100 nl of concentrated virus stock was delivered. The monoclonal anti-Gag antibody (3C2) was used to determine the spread of virus in infected embryos.

Implantation of *Noggin* Beads

Xenopus recombinant *Noggin* protein was generated and purified as described (Zimmerman *et al.*, 1996). The concentration of purified *Noggin* was in the range of 0.9–1 $\mu\text{g}/\mu\text{l}$. Thirty Affi-Blue gel beads (Bio-Rad, 75–150 μm) were rinsed five times with PBS, incubated in 1 μl of *Noggin* solution at room temperature for 2 h, and kept on ice until implantation. All *Noggin*-containing beads were freshly prepared on the day of the experiment. A single bead was implanted per embryo with the following exceptions: two or three beads were implanted in order to increase the dose of *Noggin* for generating a canal phenotype at E7, and three or four beads were implanted for generating phenotypes in the sensory structures. Beads soaked in 1 μl of BSA (1 $\mu\text{g}/\mu\text{l}$) or *Noggin*-coated beads that were immersed in 3 μl of recombinant human BMP4 solution (337 $\mu\text{g}/\text{ml}$, Genetics Institute) before implantation were used as controls. No phenotypes were induced by implantation of either type of control bead.

Embryo Processing

Infected or implanted embryos were sacrificed at different stages and processed for paint injection as described (Martin and Swanson, 1993; Bissonnette and Fekete, 1996). For analysis of sensory organs, dissected membranous labyrinths were stained with anti-HCA antibody (hair cell antigen) as described (Wu *et al.*, 1998).

In situ hybridization and preparation of riboprobes for *Bmp4*, *Msx-1*, *p75NGFR*, and *Lunatic fringe* (*Fng*) were performed as described (Wu and Oh, 1996).

BrdU Labeling and TUNEL Detection

For the detection of cell proliferation, 5-bromo-2'-deoxyuridine (BrdU) labeling solution (3 mg/ml) was applied directly onto embryos (E4–E6) *in ovo* for 3 h and then sacrificed. Embryos were fixed and processed for cryostat sectioning. Adjacent sections were used for BrdU or Terminal dUTP Nuclear End Labeling (TUNEL) staining. BrdU staining was done according to the manufacturer's procedures (Cell Proliferation Kit, Amersham). For detection of cell death, Apoptag Plus (S7101-Kit, Oncor) was used.

For E8–E9 embryos, proliferating cell nuclear antigen (PCNA) antibody (SC-56, Santa Cruz Biotechnology Inc.) was used to stain proliferating cells.

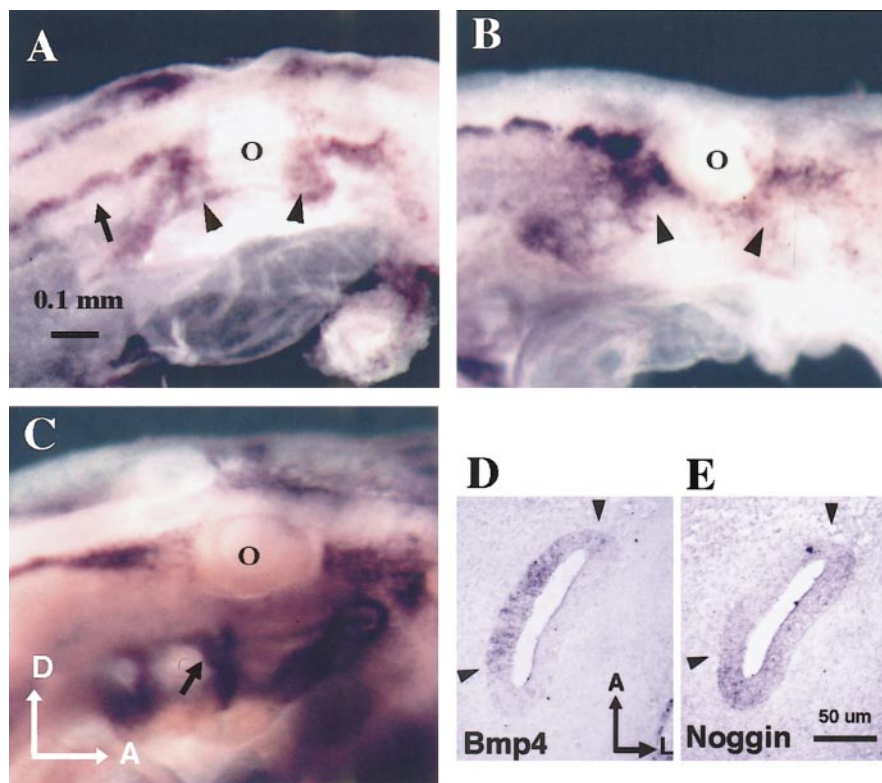


FIG. 1. Gene expression of *Noggin* in the chicken inner ear. At the otic cup stage, st14 (A) and st16 (B), *Noggin* expression can be seen in tissues flanking the otic cup (arrowheads). No expression in the epithelium of the otic cup (A, B) or otocyst (C, E2.5, st18) is detected. The absence of hybridization signal in the otocyst was further confirmed by sectioning embryos after whole-mount *in situ* hybridization. Arrow points to expression in somites in (A) and branchial arches in (C). At E4.5 (E4, st24), *Noggin* transcripts are detected in the latero-ventral portion of the basilar papilla (arrowheads, E); this region is nonoverlapping with the *Bmp4* expression domain (arrowheads, D). D and E are 12- μ m adjacent sections. O, otic cup or otocyst. Orientations: A, anterior; D, dorsal; L, lateral. Scale bar in A applies to B and C. Scale bar in E applies to D.

RESULTS

Expression of Noggin in the Chicken Inner Ear

Noggin expression was restricted in the developing inner ear. At the otic cup stage (E2, st14–16), *Noggin* was expressed in tissues surrounding the otic cup (arrowheads, Figs. 1A and 1B), and this expression became undetectable at the otocyst stage (E2.5, st18–19, Fig. 1C). Starting at E4, *Noggin* was expressed weakly in the ventral tip of the cochlear duct, in a region that was nonoverlapping with the sensory region expressing *Bmp4* (Figs. 1D and 1E); this expression remained at least until E6.5. In contrast, *Bmp4* expression is first observed in a broad domain at the early otic cup stages (Wu and Oh, 1996). By the otocyst stage, *Bmp4* is expressed in each presumptive sensory organ as well as in the mesenchyme surrounding the anlagen for the semicircular canals (Wu and Oh, 1996; Oh *et al.*, 1996). Therefore, as an antagonist of BMP4, exogenous *Noggin* could potentially interfere with BMP4 functions in the development of sensory as well as nonsensory structures.

Inner Ear Phenotypes Induced by Exogenous Noggin

A replication-competent avian sarcoma virus encoding chicken *Noggin* (RCAS-N) was injected into the lumen of otocysts at E2.5 to E3 (st18–19) and embryos were harvested at E7 or E9. Inner ears were filled with paint to reveal the gross anatomy of the membranous labyrinth (Martin and Swanson, 1993). The efficiency of viral infection was monitored by staining tissue sections with a monoclonal antibody, 3C2, directed against the viral Gag protein. Robust staining in the mesenchyme was observed 2 days postinfection, while staining within the otic epithelium was variable. The selective resistance of the otic epithelium to RCAS infection was also observed using RCAS virus encoding *Noggin* cDNA cloned in the reverse orientation or other unrelated cDNAs.

Phenotype at E7. Phenotypes of RCAS-N-infected inner ears that were harvested at E7 are summarized in Figs. 2 and 3A. At E7, the gross anatomy of a normal membranous labyrinth is fairly well formed and includes an endolym-

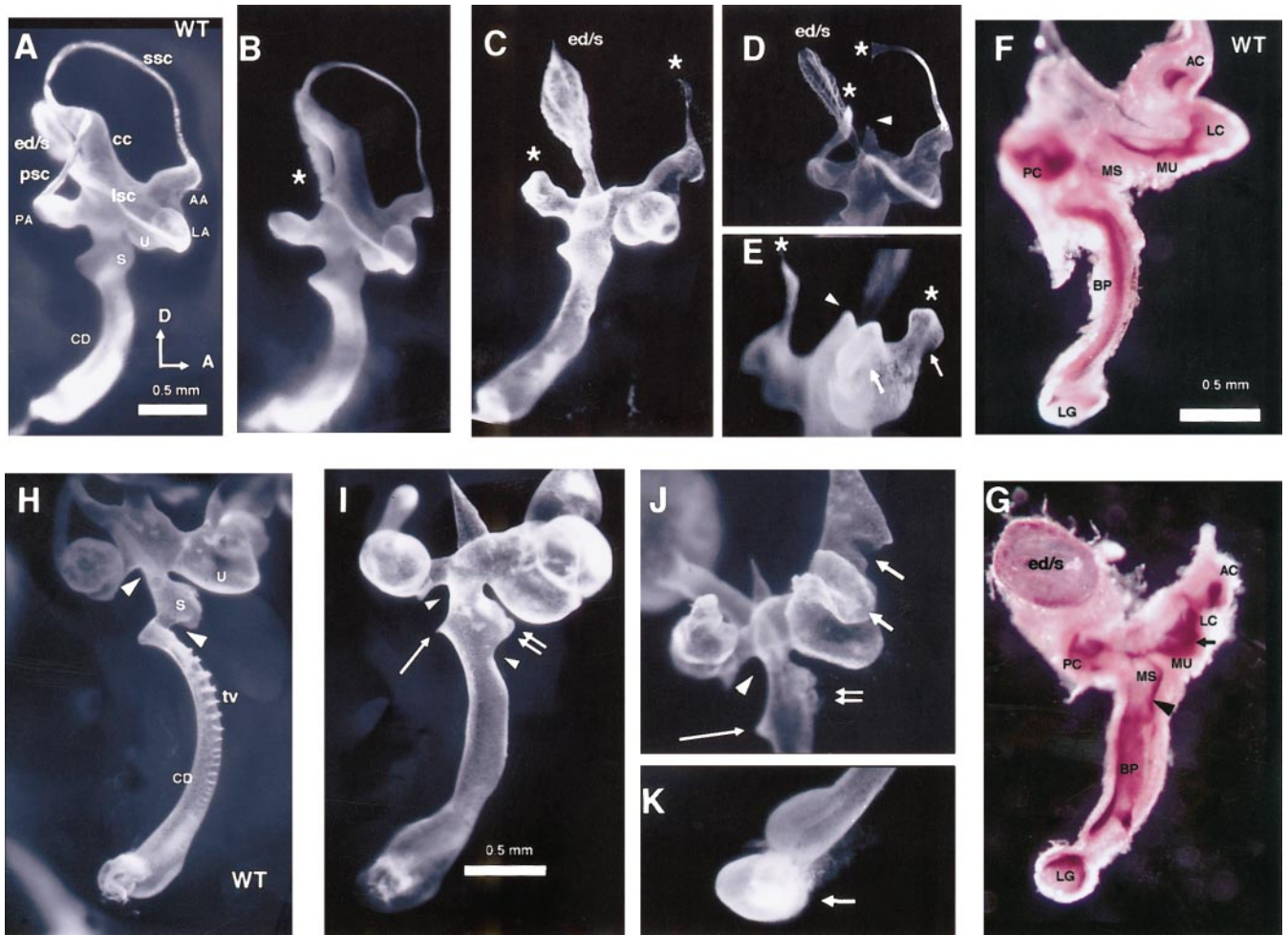


FIG. 2. RCAS-N-infected inner ears at E7 (B-E) and E9 (G, I-K). Lateral views of the membranous portion of right inner ears that were either filled with paint (A-E, H-K) for gross anatomy or stained with anti-HCA antibodies to reveal each sensory organ (F-G). (A) Normal inner ear at E7. (B) Absence of the posterior canal (asterisk). (C) Partial loss of the superior canal and complete loss of the common crus and the posterior and lateral canals (asterisks). (D) Partial loss of the common crus (arrowhead) and the superior and posterior canals (asterisks). (E) Complete loss of the superior (asterisk) and lateral canals (not marked); partial loss of the common crus (arrowhead), the posterior canal (asterisk), and the anterior and lateral ampullae (arrows). (F) Normal inner ear at E9 stained with anti-HCA. (G) RCAS-N-infected inner ear at E9. Sizes and shapes of the sensory patches are affected. The lateral crista (LC) and the macula utriculi (MU), and the macula sacculi (MS) and the basilar papilla (BP), are juxtaposed or may be fused to each other (arrow and arrowhead). However, the total number of sensory organs and their relative positions to each other are maintained ($n = 9$). (H) Partial view of normal inner ear at E9; the connections between the utricle and the saccule (utrículosaccular duct, arrowhead) and between the saccule and the cochlea (cochleosaccular duct, arrowhead) are more restricted than at E7 (A). (I-K) RCAS-N-infected ears at E9. (I) The utrículosaccular duct and the cochleosaccular duct are not restricted (arrowheads). The saccule is not fully formed (double arrows); the cochlear duct (CD) is distorted, and the proximal portion of the cochlea is poorly defined (long arrow). The distinctive demarcations in the tegmentum vasculosum (tv) are missing. (J) Only the utrículosaccular duct is apparent (arrowhead); the cochleosaccular duct is missing. The proximal tip of the cochlea is poorly defined (long arrow); the saccule (double arrows) and the anterior and lateral ampullae (arrows) are malformed. (K) The lagena is enlarged (arrow). AA, anterior ampulla; AC, anterior crista; cc, common crus; ed/s, endolymphatic duct and sac; LA, lateral ampulla; LG, lagena; lsc, lateral semicircular canal; PA, posterior ampulla; PC, posterior crista; psc, posterior semicircular canal; S, saccule; ssc, superior semicircular canal; U, utricle. See legend to Fig. 1 for orientations. Scale bar in A applies to B-E, scale bar in F applies to G, and scale bar in I applies to H-K.

phatic duct and sac (ed/s), three semicircular canals that are connected to the common crus (cc) at one end and terminate in a bulge-like structure known as the ampulla at the

other, the utricle (U), the saccule (S), and a cochlear duct (CD) (Fig. 2A). Infected inner ears displayed a range of defects involving the semicircular canals, common crus,

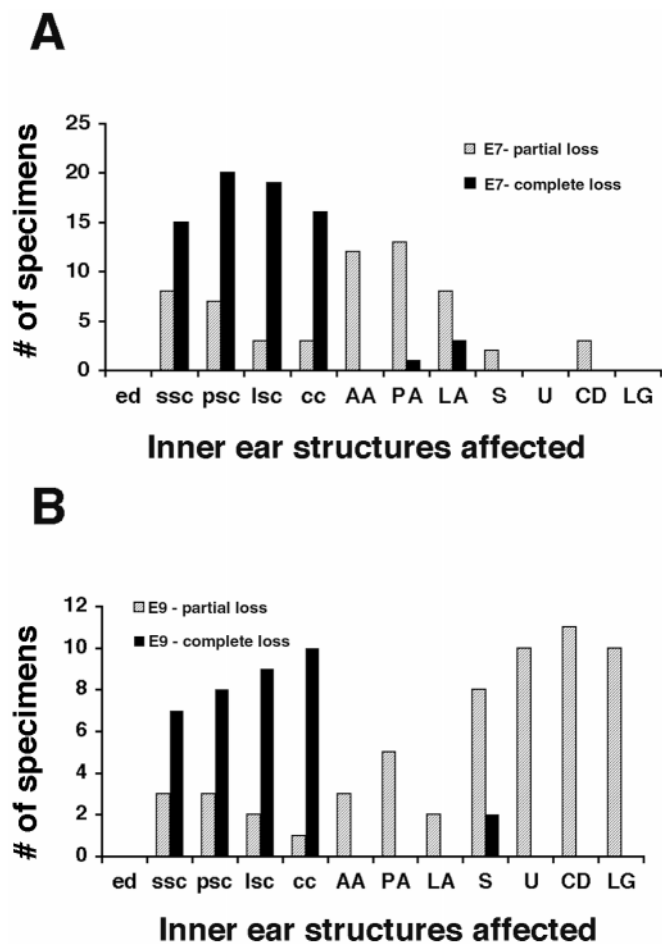


FIG. 3. Distribution of structures affected in RCAS-N infected inner ears at E7 (A, $n = 32$) and E9 (B, $n = 12$). Individual structures in each specimen were scored as normal, partial loss, or complete loss. Semicircular canals were the predominant structures affected at E7 (A), and most defects in ampullae are partial. By E9 (B), there is an increase in the number of partially affected ventral structures such as the utricle, saccule, and cochlea duct. Endolymphatic duct and sac are apparently not affected in either E7 or E9 inner ears. See legend to Fig. 2 for abbreviations.

and ampullae. Among 32 inner ears scored, the semicircular canals (ssc, psc, lsc) were most sensitive to RCAS-N treatment, whereas the endolymphatic duct and sac (ed/s) were the most resistant structures (Figs. 2B–2E and 3A). Inner ears with defects in a single canal (asterisk, Fig. 2B), or multiple canals including the common crus (asterisks and arrowhead, Figs. 2C, 2D, and 2E) were identified. However, there were no inner ears with intact semicircular canals but a defective common crus. Ampullae were also affected to varying degrees (Fig. 2E; and AA, PA, LA in Fig. 3A), but again there were no inner ears with defective ampullae and normal canals (Figs. 2D and 2E). These partially defective ampulla structures suggested that the shape and size of the

sensory tissue within the ampulla, the crista, might also be compromised (arrows, Fig. 2E and see below; E9 phenotype, arrows in Fig. 2J). Ventral inner ear structures such as the utricle, saccule, and cochlea duct were relatively unaffected at this stage (Figs. 2B, 2C, and 3A). Infection with control virus of RCAS encoding Noggin cDNA cloned in a reverse orientation did not produce any apparent phenotype.

Phenotype at E9. The phenotype of RCAS-N-infected inner ears that were infected at E2.5–E3, and harvested at E9 are summarized in Figs. 2 and 3B ($n = 12$). In addition to defects described for E7, inner ears harvested at E9 showed more extensive malformations of ventral structures such as the utricle, saccule, cochlear duct, and lagena (Fig. 3B). In normal inner ears, the connections between the utricle and the saccule, as well as between the saccule and the cochlea, become distinct by E9 (compare Figs. 2A and 2H). In RCAS-N-infected inner ears, these connections were not restricted and remained broad (arrowheads, compare Figs. 2I and 2J with 2H). The shape of the saccule was also often affected (double arrows, Figs. 2I, 2J, and 3B). In wild-type paint-filled inner ears at E9, the tegmentum vasculosum, a nonsensory component of the cochlear duct, exhibited distinct folds and troughs (tv in Fig. 2H). These structures were reduced or absent in RCAS-N-infected inner ears (Fig. 2I). In addition, the diameter and curvature of the cochlear duct were frequently affected (compare Figs. 2I and 2J with 2H). The proximal portion of the cochlear duct (long arrow in Figs. 2I and 2J) was poorly defined, and the distal portion that houses the lagena was often malformed and enlarged (Figs. 2K and 3B).

Despite these defects, the remaining structures of the membranous labyrinths at E7 or E9 showed no changes in the overall patterning. The shapes and angles of the remaining semicircular canals were correct (Figs. 2B and 2D). In Noggin-treated ears, all of the sensory organs were present and their relative positions were normal based on anti-hair cell antigen (HCA) staining. However, the structures of the individual sensory organ were misshaped, and some sensory organs may be fused (Figs. 2F and 2G, also see below).

Mechanisms of Semicircular Canal Malformation

Semicircular canal formation in the chicken inner ear can be divided into four stages: (1) outgrowth, (2) patterning, (3) resorption, and (4) continual growth. The anterior and posterior canals are both derived from the vertical outpouch, and the lateral canal is derived from the horizontal outpouch. The vertical pouch starts to form around E3.5. At E5.5, the presumptive posterior canal, via differential growth, is positioned at an approximately right angle to the presumptive anterior canal (Fig. 4A; Bissonnette and Fekete, 1996). Starting at E6, the opposing epithelia from each outpouch come together and form a fusion plate, which later “resorbs,” leaving behind a canal (Fig. 4C; Bissonnette and Fekete, 1996; Fekete *et al.*, 1997). The process of resorption is not totally understood and involves programmed cell death and possibly retraction of epithelial

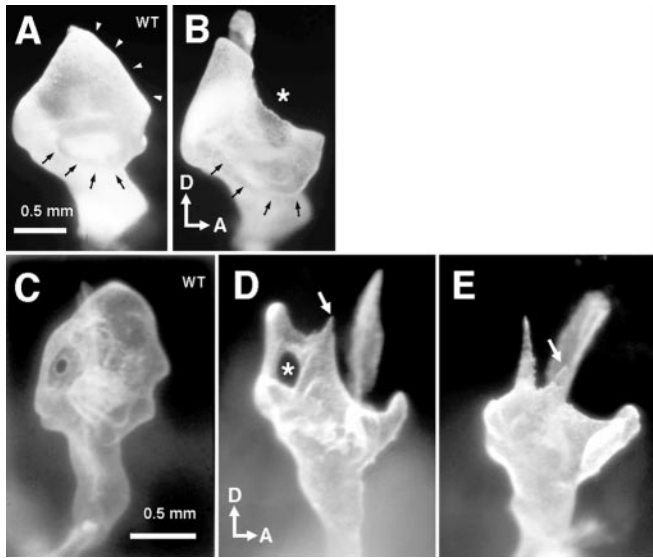


FIG. 4. Paint-filled inner ears at E5 (A, B) and E6 (C, D, E). (A, C) Normal inner ears (WT). RCAS-N-infected inner ears at E5 (B) and E6 (D, E). (B) A defect in the canal pouch is evident at E5 (asterisk, $n = 12$). (D, E) Loss of the presumptive canal plates and common crus (arrow) at E6 ($n = 14$). Small arrowheads and arrows in A and B point to the presumptive superior and lateral canal regions, respectively. An apparently normal resorption process can be seen in the specimen shown in D (asterisk). Scale bar in A applies to B. Scale bar in C applies to D and E.

cells (Martin and Swanson, 1993; Fekete *et al.*, 1997). By E7, the three semicircular canals have acquired the mature pattern but the size of the canals continues to increase until E16 (Bissonnette and Fekete, 1996).

Based on these normal developmental processes, the malformed canals of RCAS-N-infected inner ears observed at E7 could be due to a defect in the primary outgrowth of the canal pouch and/or resorption. To address this question, infected inner ears were harvested at intermediate stages. A defect in the canal plate was evident as early as E5, indicating that Noggin affected the primary outgrowth of the canal pouch (Figs. 4A and 4B). At E6 to E6.5, a reduction in the size of the canal pouch was more extensive, expanding into the presumptive common crus area (arrows, Figs. 4D and 4E). The normal resorption process that occurs in the center of the canal plate at this stage seemed to be progressing normally in the infected inner ears (asterisk, Fig. 4D).

Noggin beads mimicked RCAS-N-induced phenotypes. Phenotypes induced by RCAS-N were reproducible with the implantation of beads coated with *Xenopus* recombinant Noggin protein into mesenchymal tissue surrounding the otocyst around E3.5 to E4 (compare Fig. 5B with Fig. 2B). The size reduction in the canal pouch was observed by 24 h after implantation (Fig. 5A). Implantation of Noggin beads

to either the anterior or the posterior side of the otocyst resulted in inner ear defects in closest proximity to the beads. Noggin beads implanted in the lumen of the otocysts were not as potent in eliciting a phenotype as beads implanted in the surrounding mesenchyme (data not shown). Localized defects were also attainable with RCAS-N when virus was injected into a single location within the otic mesenchyme instead of the lumen of otocysts.

Noggin reduced proliferation of canal outpouch. Since the location and delivery of exogenous Noggin can be better controlled using Noggin beads instead of RCAS-N, we used the bead implantation approach to address mechanisms underlying the canal outpouch defect. Following bead implantation into the mesenchyme by the anterior region of otocysts, inner ears were analyzed for proliferation using BrdU labeling and programmed cell death using TUNEL staining. Analysis of BrdU-labeled cells in otic epithelia was done at 6, 12, and 24 h post-Noggin bead implantation (Figs. 5D, 5E, and 6A). BrdU-labeled cells were scored in two sections dorsal to the level where the endolymphatic duct joins the utricle (dotted line, Fig. 5C). Labeled cells in the anterior half of the inner ear on the Noggin-implanted side were counted (straight line, Fig. 5E). Comparable sections and areas from the nonimplanted inner ear (left ear) were counted as control. The difference in total counts between control and treated sides of each embryo were calculated and a paired *t*-test was conducted. At all time points tested, there was a significant decrease in BrdU labeling in treated ears compared to controls (6 h, 35 ± 23.4 ; 12 h, 65.5 ± 33.4 ; 24 h, 60.4 ± 43.9 ; value represents the mean of the difference \pm 95% confidence interval for the mean; $n = 4$). The number of BrdU-labeled cells from treated ears is expressed as the percentage of control and is summarized in Fig. 6A. Representative sections at 12 h postimplantation are illustrated in Figs. 5D and 5E. In addition, since the 12-h time point showed the most reduction in BrdU labeling (Fig. 6A), in a more thorough analysis, all sections in the presumptive superior canal region were counted in treated and control specimens. Total counts were grouped as dorsal, middle, and ventral regions and compared to controls, and the results show a significant difference between control and treated embryos in all three groups (dorsal region, 13 ± 9.2 ; middle region, 63.5 ± 32.3 ; ventral region, 89.75 ± 45.1 ; value represents the mean of the difference \pm 95% confidence interval for the mean; $n = 4$).

Noggin induces apoptosis in canal pouch as a late effect. Alternate sections from the same inner ears described above were processed for TUNEL staining. The numbers of apoptotic cells were determined by counting TUNEL-positive cells of all sections from the presumptive superior canal region (straight line, Fig. 5E), and the results are summarized in Fig. 6B. At 24 h postimplantation, a reduction in the thickness of the otic epithelium in the implanted side was observed ($n = 4$, arrow in Fig. 5F). No apoptosis, however, was evident in the epithelium at this

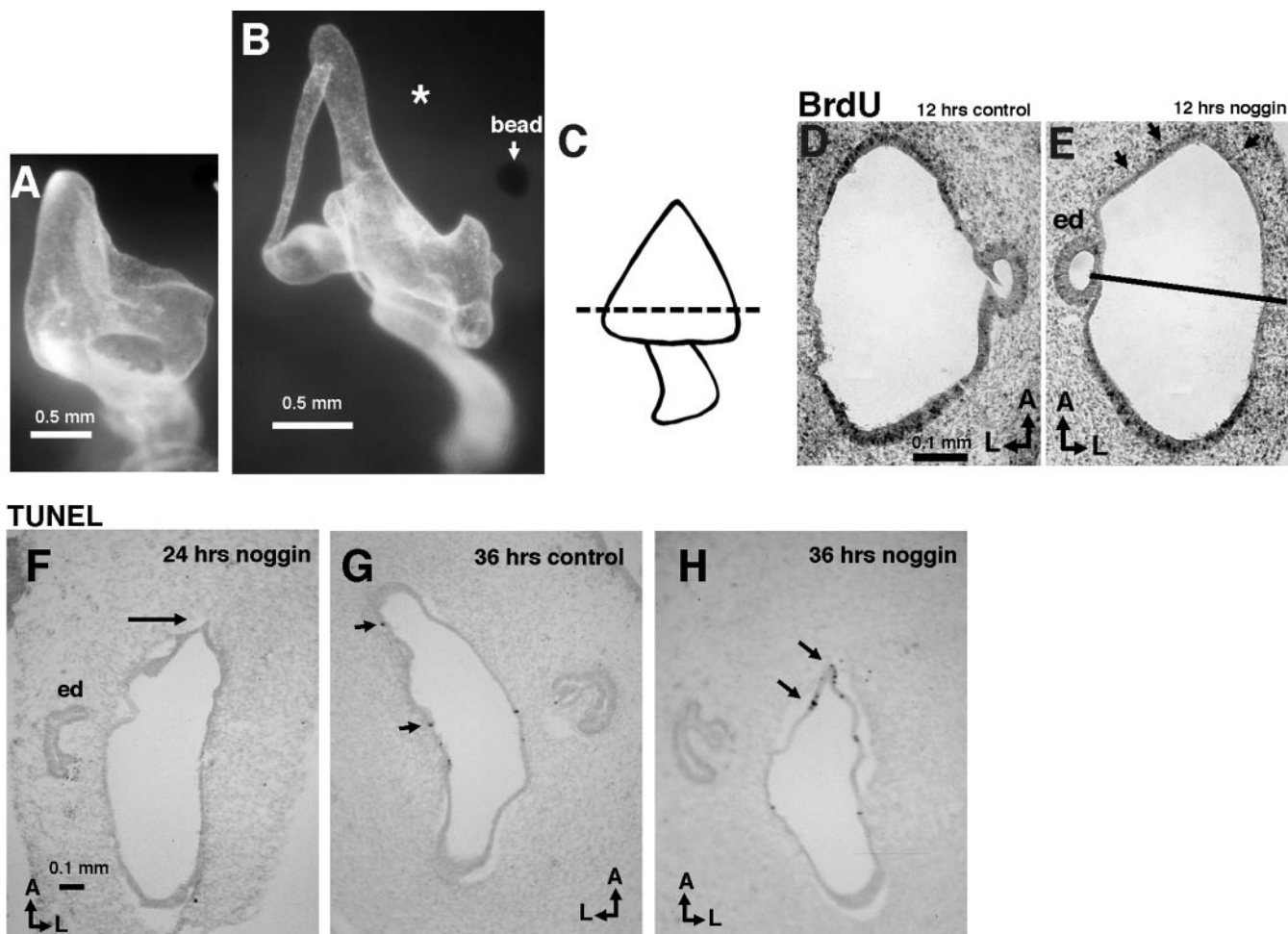


FIG. 5. Phenotypes of Noggin bead-implanted inner ears. Beads were implanted in the mesenchyme by the anterior portion of the otocyst in all panels shown. Noggin bead-implanted inner ears at 24 h (A, E5, $n = 3$) and 3 days (B, E7, $n = 14$) after implantation. Asterisk indicates an absence of a superior canal (B). (C) A schematic illustrating the approximate level of sections used for scoring BrdU- and TUNEL-labeled cells. Representative sections of BrdU labeling from control (D) and implanted (E) sides of the same embryo at 12 h postimplantation are shown. Reduction of labeling can be seen at the anterior portion of the otic epithelium at the implanted side (small arrows, E). The straight line demarcates the anterior portion of the otic epithelium that was scored for BrdU and TUNEL labeling. (F–H) Representative sections stained with TUNEL at 24 h (F, implanted side) and 36 h (G, control side; H, implanted side) post-Noggin implantation. No TUNEL-labeled cells were detected in the canal pouch at 24 h but changes in the morphology of the otic epithelium are evident (arrow, F). G and H are comparable sections from the same embryo. At 36 h postimplantation, the normal inner ear shows few apoptotic cells in that region (arrows in G), whereas apoptotic cells are frequently observed in Noggin-treated ears (arrows in H). The presumptive superior canal area is reduced in size (H). ed, endolymphatic duct. See legend to Fig. 1 for orientations. Scale bar in D applies to E, and scale bar in F applies to G and H.

stage. By 36 h postimplantation (E5 to E5.5), apoptotic cells in control inner ears were sparse (arrows, Figs. 5G and 6B), whereas in the Noggin-treated inner ears, apoptotic cells were observed frequently (arrows, Figs. 5H and 6B; $n = 4$). The size of the canal pouch was also reduced by the site of bead implantation (Figs. 5G and 5H). Taken together, the BrdU labeling and TUNEL staining results show that reduction in cell proliferation is the primary cause for the defects observed in the canal outpouch at 24 h, followed by an increase in apoptosis at 36 h postimplantation (Figs. 5A and 6).

Noggin Affects the Continual Outgrowth of Formed Semicircular Canals

In addition to examining effects of Noggin during canal formation, we investigated the effect of Noggin on the continual outgrowth of the canals after their formation at E7. Implantation of two or three Noggin-soaked beads to E7 or E7.5 inner ears resulted in the absence or occlusion of the canal 2 days postimplantation ($n = 9$, Fig. 7A). Control beads coated with bovine serum albumin had no effect. Embryos implanted for either 1 ($n = 3$) or 2 days ($n = 3$) were

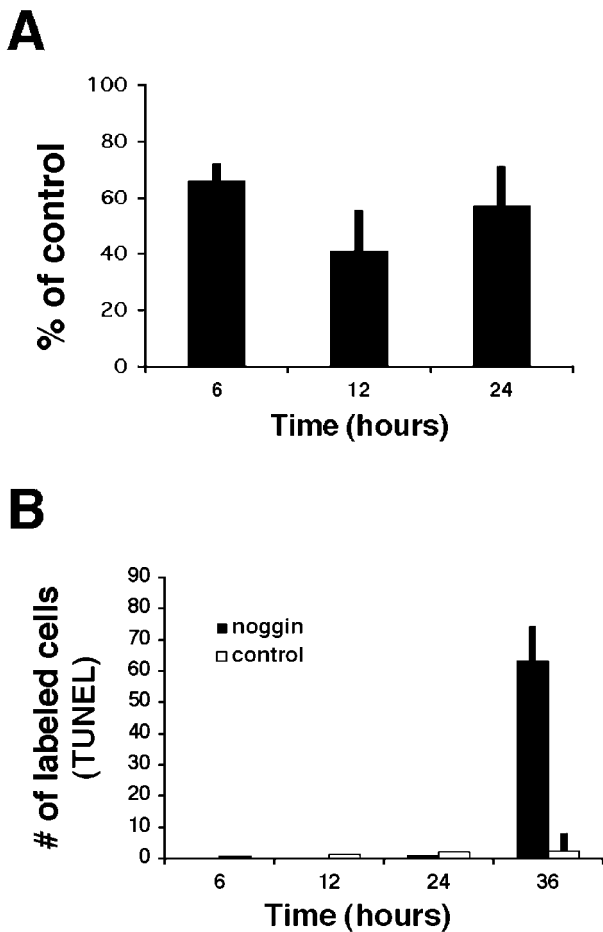


FIG. 6. Histograms of BrdU (A) and TUNEL (B) labeling in inner ears implanted with Noggin beads. (A) BrdU-labeled cells in Noggin-treated ears are expressed as percentages of controls at 6, 12, and 24 h after implantation. (B) Total number of TUNEL-positive cells in the anterior presumptive canal region of control and treated ears at 6, 12, 24, and 36 h postimplantation. Bar represents standard error of the mean ($n = 4$).

FIG. 7. Noggin effects on formed canals. (A) A paint-filled inner ear showing canal defects 2 days after Noggin implantation at E7 ($n = 9$). Arrowhead points to an intact common crus. However, portions of both the superior and the posterior canals adjacent to the two implanted beads were affected (asterisk). (B) PCNA staining of a normal canal at E9 is restricted (arrows). (C) Noggin-treated canal is disorganized and shows diffuse PCNA staining. (D–G) Gene expressions of normal and treated canals at E9 ($n = 3$). D and E as well as F and G are 12- μm adjacent sections. D and E are control sections (left ear) selected from regions comparable to F and G (right ear) of the same embryo. At E9, the expression domains of *Bmp4* (D) and *Msx1* (E) in normal canals are restricted (arrows). In Noggin-treated ears, *Bmp4* expression is normal or may be slightly increased (F), whereas *Msx1* expression is greatly reduced (asterisk, G). There is an increase of *Bmp4* expression in cells in the immediate vicinity of the bead (asterisk, F) which is located in the upper left hand corner of F and G. See legend to Fig. 2 for abbreviations. Scale bar in B applies to C, scale bar in D applies to E–G.

FIG. 8. Effects of Noggin-implanted beads on sensory organ formation. (A) Normal paint-filled inner ear harvested at E9. (B) Noggin beads implanted to the antero-medial portion of the inner ear at E4.5. At E9, in addition to the absence of the superior canal, the anterior ampulla (arrow), the utricle (arrowhead), and the saccule (asterisk) are partially defective. (C–F) Dissected sensory organs stained with anti-HCA as wholemounts. (C) A normal anterior crista in frontal view showing a W-shaped pattern of staining; this pattern is lost in Noggin-treated ears (D). (E) Normal macula utriculi showing a relatively flat sensory organ with stronger HCA staining in the periphery; this sensory organ is smaller and appears collapsed in the treated inner ears (F). Scale bar in A applies to B, and scale bar in D applies to C, E, and F.

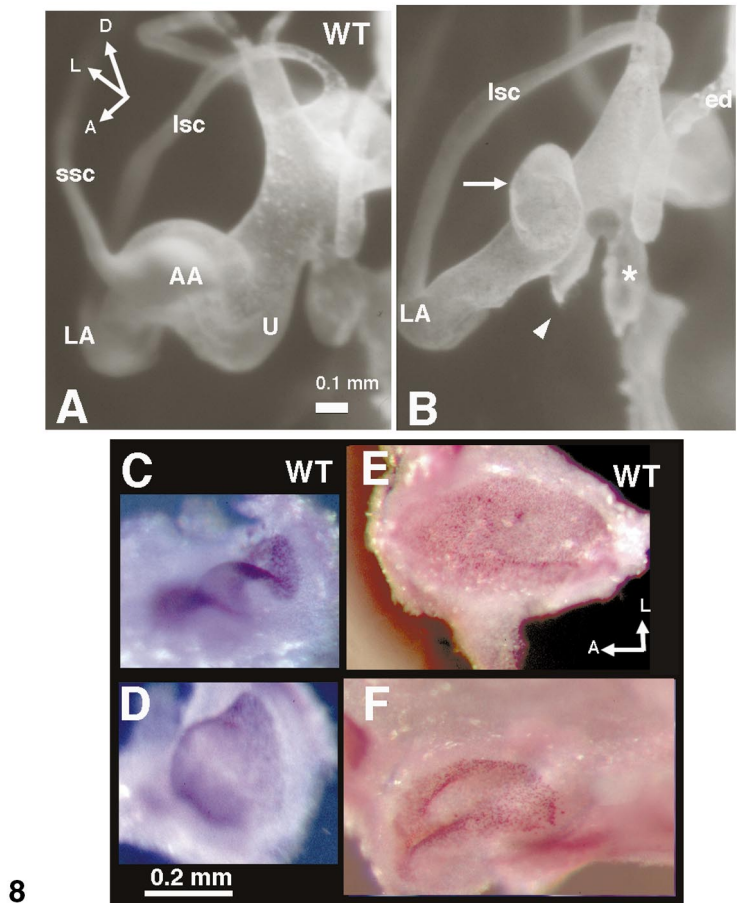
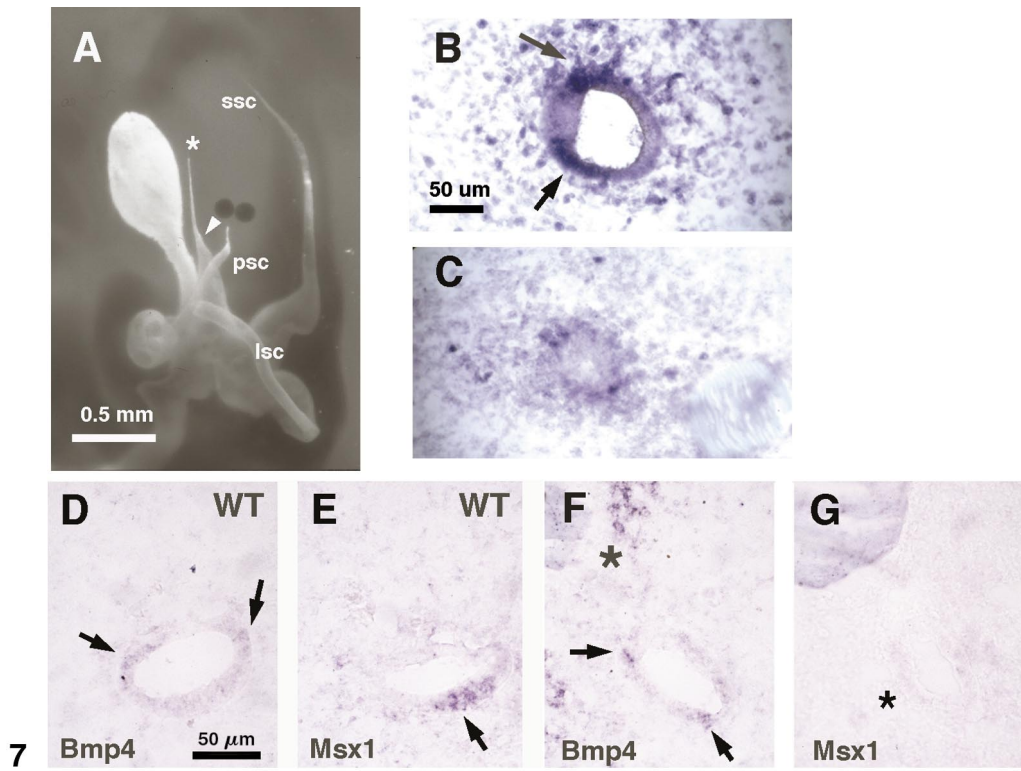
used to examine the effect of Noggin on proliferation and cell death. The inner ears were paint filled and photographed before processing for proliferating cell antigen (PCNA) antibody or TUNEL staining for the detection of proliferating cells or programmed cell death, respectively. The affected canals were identified by their proximity to the implanted beads. Normal canals exhibited PCNA staining as two foci (arrows, Fig. 7B), whereas affected canals showed a diffused staining pattern by 1 day and a disorganized histology by 2 days postimplantation (Fig. 7C). TUNEL staining revealed that apoptotic cells were sparse in canals at this stage, with no significant difference between control and treated canals at either 1 or 2 days postimplantation (data not shown).

In a normal canal at E9, *Bmp4* and *Msx1* are expressed in distinct regions within the canal epithelium (arrows, Figs. 7D and 7E). In canals exposed to Noggin, *Bmp4* expression in the canal epithelium was normal or slightly increased (arrows, Fig. 7F). In the mesenchyme, however, the increase in *Bmp4* expression surrounding the bead was dramatic (asterisk, Fig. 7F). In contrast, *Msx1* expression in the canals was greatly decreased (asterisk, Fig. 7G).

Noggin Affects Sensory Organ Formation

The effect of Noggin on sensory organ formation was examined at E4.5–5, a stage when each presumptive sensory organ is a distinct entity based on *Bmp4* expression (Wu and Oh, 1996). Noggin beads were implanted in the mesenchyme near the antero-medial portion of the inner ear. Implanted embryos were harvested at E9 or E10 for paint injection or HCA whole-mount staining. Some embryos were also harvested 1 or 1.5 days after implantation for gene expression studies.

Under these experimental conditions, the anterior ampulla and the utricle were most proximal to the bead and thus the most prevalent sensory structures affected (9 of 10 specimens; arrow and arrowhead in Figs. 8A and 8B). Results from paint-filled Noggin-treated inner ears suggested that the development of the sensory structures



might also be compromised (Figs. 2E, 2J, and 8B). To directly examine the sensory structures, anti-HCA antibodies were used. Anti-HCA staining of sensory organs showed that the pattern of crista was indeed affected rather than just reduced in size. The normal W-shaped pattern of the anterior crista was disrupted (8 of 9 specimens; Figs. 8C and 8D). The pattern of the macula utriculi was also smaller and appeared collapsed (Figs. 8E and 8F).

The changes in size and shape of the sensory organs may ultimately be due to changes in gene expression. Alternatively, the failure of normal sensory organ formation may be less direct and due to physical constraints resulting from abnormal development of the adjacent epithelium. Four established markers for the presumptive cristae were examined, *Bmp4*, *Fng*, *p75NGFR*, and *Msx1* (Wu and Oh, 1996; Oh et al., 1996; Adam et al., 1998). *Msx-1* and *p75NGFR* expression was decreased in the presumptive anterior crista within 24 and 36 h of bead implantation (24 h, $n = 7$; 36 h, $n = 4$; arrows in Figs. 9B and 9D). However, *Bmp4* and *Fng* expression remained unchanged (AC, Figs. 9A and 9C), and their expressions served as markers for the location of the affected cristae. While *Msx1* expression was lower than normal in the anterior crista, its expression in the endolymphatic duct remained unchanged (ed/s, Fig. 9D). Levels of expression of these four genes in the presumptive posterior cristae were normal (PC, Fig. 9). Also, inner ears implanted with beads coated with BSA showed no change in any of the four markers examined. These results suggest that Noggin has a direct effect on crista formation.

DISCUSSION

Noggin-Induced Phenotypes Likely Result from Blocking BMP4 Function

In tissues such as the neural tube, limbs, and somites, *Noggin* is expressed in restricted domains that are usually complementary to *Bmp* expressing domains. The opposing functions and relative concentrations of *Noggin* and BMPs in these organs act in conjunction to mediate their proper formation (McMahon et al., 1998; Brunet et al., 1998; Capdevila and Johnson, 1998; Reshef et al., 1998; Marcelle et al., 1997). In the inner ear, such a coordinated role for BMPs and *Noggin* is not readily apparent since *Noggin* transcripts were not detected in the epithelium of the otic cup or otocyst. However, the transient endogenous expression of *Noggin* in tissues surrounding the otic cup could potentially modulate BMP activities in the otic epithelium and mediate proper inner ear development. In addition, the low level of *Noggin* transcripts in the ventral portion of the developing cochlea could also modulate BMP activities in that region (Figs. 1D and 1E). Consistent with this hypothesis, the ventral portion of the cochlea was usually affected by *Noggin* treatment (LG in Fig. 3B).

Regardless of the endogenous role of *Noggin* in the early development of the chicken inner ear, the majority of the phenotypes observed in this study most likely reflect a

direct impediment of endogenous BMP4 activity. In support of this supposition, at the later times of development when *Noggin* was experimentally applied, no endogenous *Noggin* was expressed in most of the structures that were ultimately affected. Therefore the exogenous *Noggin* is not merely augmenting endogenous function. Furthermore, all of the structures that were affected invariably express *Bmp4*. It should be noted that these structures also express *Bmp7* (Oh et al., 1996). Therefore, even though *Noggin* binds BMP7 at a much lower affinity than BMP4, we cannot rule out the possibility that *Noggin* also blocks the function of BMP7 (or other BMPs and their heterodimers) (Zimmerman et al., 1996). It is noteworthy that the endolymphatic duct and sac, which were not affected by *Noggin* treatment, express *Bmp7* but not *Bmp4* (Oh et al., 1996), suggesting that *Noggin* is unlikely to block BMP7 directly within the inner ear. BMP2, which binds *Noggin* with affinity equivalent to BMP4, was not detected in the developing otocyst by either *in situ* hybridization or RT-PCR techniques (unpublished results). Therefore, BMP2 is unlikely to be a target of *Noggin* in these experiments.

RCAS-N-infected inner ears showed more extensive phenotypes than *Noggin* bead-implanted ears, which was attributed to a continuation as well as widespread delivery of *Noggin* protein by virally infected cells. The phenotypes induced by exogenous *Noggin*, delivered by either method, however, were best interpreted as a local source of *Noggin* protein that blocked normal BMP4 signaling in that region, while leaving the rest of the inner ear structures relatively unperturbed. There are three primary sources of BMP4 within the developing inner ear; *Bmp4* is initially expressed in the presumptive sensory patches and then later in the surrounding mesenchyme and canals. Both the extent of diffusion of BMP4 from these sources and the responsive cells are not defined. For example, BMP4 secreted by the epithelial cells could act in a cell-autonomous fashion, as well as affect adjacent epithelial or mesenchymal cells. Therefore, even though delivery of *Noggin* to the mesenchyme appeared to be more efficient in eliciting a phenotype than delivery to the lumen of the otocysts, it is difficult to distinguish which source(s) of BMP4 is being depleted by *Noggin*. At this point, we favor the interpretation that *Noggin* is blocking all three sources of BMP4 based on the observation that *Noggin* induced changes in gene expression in all three locations (Figs. 7 and 9).

An increase of *Bmp4* gene expression was often observed in the tissues surrounding *Noggin* beads (Fig. 7F), even though the available BMP4 protein was most likely depleted by the presence of *Noggin*. This increase of *Bmp4* expression has been reported in other systems as well (Capdevila and Johnson, 1998; Pizette and Niswander, 1999) and most likely represents an autoregulatory pathway of *Bmp4*. It is not clear whether this increase of *Bmp4* gene expression modulated the observed phenotypes. Delivery of beads coated with BMP4 protein, however, produced a range of phenotypes unrelated to those presented here (unpublished results).

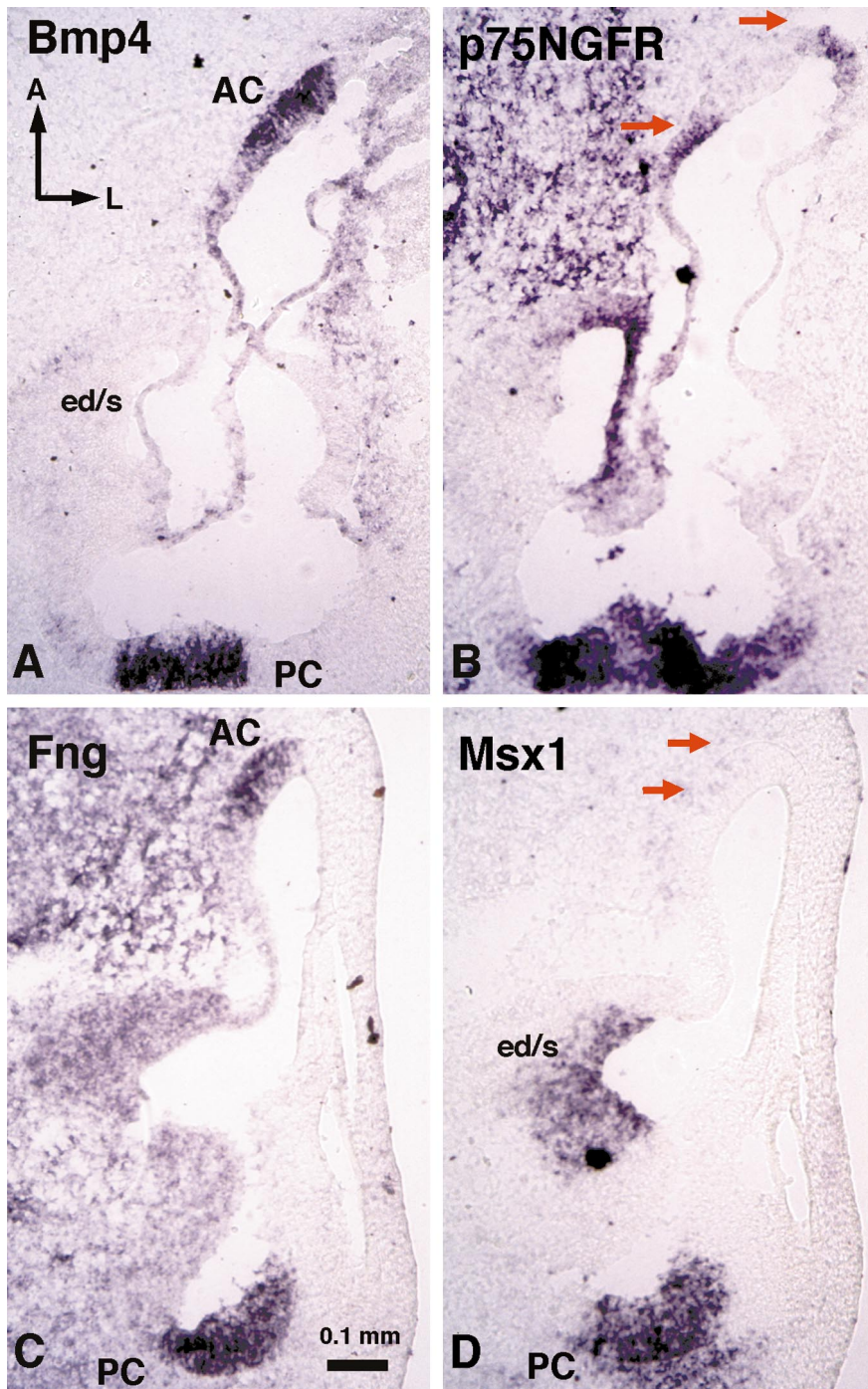


FIG. 9. *Bmp4* (A), *p75NGFR* (B), *Fng* (C), and *Msx1* (D) expression in presumptive cristae 24 h after Noggin bead implantation ($n = 7$). A Noggin bead was implanted in the antero-medial portion of the inner ear at E4.5. A and B as well as C and D are 12- μ m adjacent sections. (A) *Bmp4* is expressed in the anterior and posterior cristae (AC, PC). (B) *p75NGFR* expression is maintained in the posterior crista, but is severely reduced in the anterior crista (demarcated by red arrows). (C) *Fng* is expressed in the anterior and posterior cristae. (D) *Msx1* expression in the posterior crista and the endolymphatic duct and sac (ed/s) is maintained, but expression in the anterior crista is greatly reduced (red arrows). Scale bar in C applies to all panels.

Effects of Noggin on Nonsensory Structures

Among the nonsensory structures, the semicircular canals were most sensitive, and the endolymphatic duct and sac were the most resistant to Noggin treatment. *Bmp4* is initially expressed in the mesenchyme surrounding the presumptive canal outpouch area. Later, its expression is localized in restricted domains within the canals. Using Noggin-soaked beads, we demonstrated that BMP4 (and possibly other BMPs) is required for several phases of canal development, from the initial outpocketing stage to the continual growth of the canal after its formation. The initial defect of the canal outpouch is a result of reduced cell proliferation, followed by an increase in programmed cell death. It is not clear whether this cell death is related to the normal resorption process. However, the normal resorption process appeared to progress independently in some cases (Fig. 4D).

Effects of Noggin on Sensory Structures

Sensory structures were more resistant to Noggin treatment than nonsensory structures, based on the fact that multiple beads were required in order to elicit a phenotype in sensory structures. This could be partly due to a relatively higher level of *Bmp4* expression in the sensory versus nonsensory structures at E4 (Oh et al., 1996). Nevertheless, we demonstrated that within 24 h of Noggin treatment, expression of *p75NGFR* and *Msx1*, two presumptive crista markers, were reduced. In contrast, expression of more general sensory organ markers such as *Fng* and *Bmp4* was not affected. These results are consistent with the observation that the cristae do form in Noggin-treated ears, but their structural patterning is affected, possibly via the decrease of *Msx1* and *p75NGFR* expression. However, no apparent defects of the cristae were reported in *Msx1* knockout mice (Satokata and Maas, 1994). Due to the lack of molecular markers specific for the developing maculae of the utricle and saccule, it is difficult to evaluate whether changes in these sensory organs were also a consequence of changes in gene expression. Furthermore, *Bmp4* expression in the two maculae is transient and *Bmp4* transcripts are no longer detectable by E9, whereas *Bmp4* expression persisted until E12 in the cristae (Oh et al., 1996). In the basilar papilla, *Bmp4* expression becomes restricted to sensory hair cells. The significance of this expression for cochlear hair cell formation is not clear, and this pattern of expression is not conserved in mice (Morsli et al., 1998). Sensory hair cells seemed to form normally in Noggin-treated ears as indicated by HCA staining (Figs. 2G, 8D, and 8F) and early expression patterns of *Fng* and *Bmp4* (Figs. 9A and 9C). However, some aberrant hair cell patterns have been observed in the basilar papilla, which warrants further investigation (data not shown).

The initial broad expression of *Bmp4* transcripts at the margin of the otic cup, which becomes restricted after the otocyst is formed, suggests that *Bmp4* may play a role in specifying sensory organ type and positional information.

Experiments presented here addressed only whether *Bmp4* is required for the differentiation of sensory organs, since Noggin beads were implanted after each presumptive sensory organ was a distinct entity (based on gene expression). Preliminary experiments of implanting Noggin beads at an earlier stage suggest that the identity and positional information of some sensory organs may be compromised by Noggin treatment. Nevertheless, more sensory organ-specific markers are needed before we can verify these results. It is interesting to point out that *Msx1* expression in both cristae and canals was reduced in Noggin-treated inner ears. Both of these regions are also associated with *Bmp4* expression. In the endolymphatic duct and sac, where only *Msx1* is expressed and not *Bmp4*, *Msx1* transcription was not affected by Noggin treatment. These results suggest that *Msx1* expression in the cristae and canals may be regulated by *Bmp4*, similar to what has been reported in other systems (Zou and Niswander, 1996; Vainio et al., 1993).

Taken together, results from this study provide the first evidence that BMP4 has multiple roles in the formation of sensory and nonsensory components of the inner ear. Future experiments will focus on deciphering potential earlier roles of BMP4 in sensory organ specification.

ACKNOWLEDGMENTS

We are indebted to Dr. Randy Johnson for the gift of Noggin virus prior to publication. We also thank Dr. Guy Richardson for the anti-HCA antibodies and Drs. Susan Sullivan and Robert Fridell for critically reading the manuscript.

REFERENCES

- Acampora, D., Mazan, S., Avvantaggiato, V., Barone, P., Tuorto, F., Lallemand, Y., Brulet, P., and Simeone, A. (1996). Epilepsy and brain abnormalities in mice lacking the *otx1* gene. *Nat. Genet.* **14**, 218–222.
- Adam, J., Myat, A., Le Roux, I., Eddison, M., Henrique, D., Ish-Horowicz, D., and Lewis, J. (1998). Cell fate choices and the expression of Notch, Delta and Serrate homologues in the chick inner ear: Parallels with *Drosophila* sense-organ development. *Development* **125**, 4645–4654.
- Bissonnette, J. P., and Fekete, D. M. (1996). Standard atlas of the gross anatomy of the developing inner ear of the chicken. *J. Comp. Neurol.* **174**, 1–11.
- Brunet, L. J., McMahon, J. A., McMahon, A. P., and Harland, R. M. (1998). Noggin, cartilage morphogenesis, and joint formation in the mammalian skeleton. *Science* **280**, 1455–1457. [See comments]
- Capdevila, J., and Johnson, R. L. (1998). Endogenous and ectopic expression of noggin suggests a conserved mechanism for regulation of BMP function during limb and somite patterning. *Dev. Biol.* **197**, 205–217.
- Cho, K. W., and Blitz, I. L. (1998). BMPs, Smads and metalloproteases: Extracellular and intracellular modes of negative regulation. *Curr. Opin. Genet. Dev.* **8**, 443–449.

- Fekete, D. M. (1999). Development of the vertebrate ear: Insights from knockouts and mutants. *Trends Neurol. Sci.* **22**, 263–269.
- Fekete, D. M., Homburger, S. A., Waring, M. T., Riedl, A. E., and Garcia, L. F. (1997). Involvement of programmed cell death in morphogenesis of the vertebrate inner ear. *Development* **124**, 2451–2461.
- Fritzsche, B., Barald, K., and Lomax, M. (1998). Early embryology of the vertebrate ear. In "Development of the Auditory System, Springer Handbook of Auditory Research" (E. Rubel, A. Popper, and R. S. Fay, Eds.), pp. 81–145. Springer, New York.
- Hadrys, T., Braun, T., Rinkwitz-Brandt, S., Arnold, H. H., and Bober, E. (1998). Nkx5-1 controls semicircular canal formation in the mouse inner ear. *Development* **125**, 33–39.
- Hamburger, V., and Hamilton, H. (1951). A series of normal stages in the development of the chick embryo. *J. Morphol.* **88**, 49–92.
- Hemmati-Brivanlou, A., and Thomsen, G. (1995). Ventral mesodermal patterning in *Xenopus* embryos: Expression patterns and activities of BMP-2 and BMP-4. *Dev. Genet.* **17**, 78–89.
- Hogan, B. L. (1996). Bone morphogenetic proteins in development. *Curr. Opin. Genet. Dev.* **6**, 432–438.
- Holley, S. A., Neul, J. L., Attisano, L., Wrana, J. L., Sasai, Y., O'Connor, M. B., De Robertis, E. M., and Ferguson, E. L. (1996). The *Xenopus* dorsalizing factor noggin ventralizes *Drosophila* embryos by preventing DPP from activating its receptor. *Cell* **86**, 607–617.
- Marcelle, C., Stark, M. R., and Bronner-Fraser, M. (1997). Coordinate actions of BMPs, Wnts, Shh and noggin mediate patterning of the dorsal somite. *Development* **124**, 3955–3963.
- Martin, P., and Swanson, G. J. (1993). Descriptive and experimental analysis of the epithelial remodellings that control semicircular canal formation in the developing mouse inner ear. *Dev. Biol.* **159**, 549–558.
- McMahon, J. A., Takada, S., Zimmerman, L. B., Fan, C. M., Harland, R. M., and McMahon, A. P. (1998). Noggin-mediated antagonism of BMP signaling is required for growth and patterning of the neural tube and somite. *Genes Dev.* **12**, 1438–1452.
- Morgan, B. A., and Fekete, D. M. (1996). Manipulating gene expression with replication-competent retroviruses. *Methods Cell Biol.* **51**, 185–218.
- Morsli, H., Choo, D., Ryan, A., Johnson, R., and Wu, D. K. (1998). Development of the mouse inner ear and origin of its sensory organs. *J. Neurosci.* **18**, 3327–3335.
- Morsli, H., Tuorto, F., Choo, D., Postiglione, M. P., Simeone, A., and Wu, D. K. (1999). Otx1 and Otx2 activities are required for the normal development of the mouse inner ear. *Development* **126**, in press.
- Oh, S. H., Johnson, R., and Wu, D. K. (1996). Differential expression of bone morphogenetic proteins in the developing vestibular and auditory sensory organs. *J. Neurosci.* **16**, 6463–6475.
- Pizette, S., and Niswander, L. (1999). BMPs negatively regulate structure and function of the limb apical ectodermal ridge. *Development* **126**, 883–894.
- Reshef, R., Maroto, M., and Lassar, A. B. (1998). Regulation of dorsal somitic cell fates: BMPs and Noggin control the timing and pattern of myogenic regulator expression. *Genes Dev.* **12**, 290–303.
- Satokata, I., and Maas, R. (1994). Msx1 deficient mice exhibit cleft palate and abnormalities of craniofacial and tooth development. *Nat. Genet.* **6**, 348–356.
- Schultheiss, T. M., Burch, J. B., and Lassar, A. B. (1997). A role for bone morphogenetic proteins in the induction of cardiac myogenesis. *Genes Dev.* **11**, 451–462.
- Smith, W. C., and Harland, R. M. (1992). Expression cloning of noggin, a new dorsalizing factor localized to the Spemann organizer in *Xenopus* embryos. *Cell* **70**, 829–840.
- Torres, M., and Giraldez, F. (1998). The development of the vertebrate inner ear. *Mech. Dev.* **71**, 5–21.
- Torres, M., Gomez-Pardo, E., and Gruss, P. (1996). Pax2 contributes to inner ear patterning and optic nerve trajectory. *Development* **122**, 3381–3391.
- Urist, M. R., Mikulski, A., and Lietze, A. (1979). Solubilized and insolubilized bone morphogenetic protein. *Proc. Natl. Acad. Sci. USA* **76**, 1828–1832.
- Vainio, S., Karavanova, I., Jowett, A., and Thesleff, I. (1993). Identification of BMP-4 as a signal mediating secondary induction between epithelial and mesenchymal tissues during early tooth development. *Cell* **75**, 45–58.
- Wang, W., Van De Water, T., and Lufkin, T. (1998). Inner ear and maternal reproductive defects in mice lacking the Hmx3 homeobox gene. *Development* **125**, 621–634.
- Winnier, G., Blessing, M., Labosky, P. A., and Hogan, B. L. M. (1995). Bone morphogenetic protein-4 is required for mesoderm formation and patterning in the mouse. *Genes Dev.* **9**, 2105–2116.
- Wozney, J. M., Rosen, V., Celeste, A. J., Mitscock, L. M., Whitters, M. J., Kriz, R. W., Hewick, R. M., and Wang, E. A. (1988). Novel regulators of bone formation: molecular clones and activities. *Science* **242**, 1528–1534.
- Wu, D. K., Nunes, F. D., and Choo, D. (1998). Axial specification for sensory organs versus nonsensory structures of the chicken inner ear. *Development* **125**, 11–20.
- Wu, D. K., and Oh, S. H. (1996). Sensory organ generation in the chick inner ear. *J. Neurosci.* **16**, 6454–6462.
- Zimmerman, L. B., De Jesus-Escobar, J. M., and Harland, R. M. (1996). The Spemann organizer signal noggin binds and inactivates bone morphogenetic protein 4. *Cell* **86**, 599–606.
- Zou, H., and Niswander, L. (1996). Requirement for BMP signaling in interdigital apoptosis and scale formation. *Science* **272**, 738–741.

Received for publication July 23, 1999

Revised August 16, 1999

Accepted August 17, 1999